JACS
JOURNAL OF THE AMERICAN CHEMICAL SOCIETY
Communication
pubs.acs.org/JACS

Mechanism of Action of the Cell-Division Inhibitor PC190723: Modulation of FtsZ Assembly Cooperativity

Nathaniel L. Elsen,[†] Jun Lu,[‡] Gopal Parthasarathy,[‡] John C. Reid,[‡] Sujata Sharma,[†] Stephen M. Soisson,[‡] and Kevin J. Lumb*,[†]

[†]Screening and Protein Sciences, Merck Research Laboratories, West Point, Pennsylvania 19486, United States
[‡]Global Structural Chemistry, Merck Research Laboratories, West Point, Pennsylvania 19486, United States

Supporting Information

ABSTRACT: The cooperative assembly of FtsZ, the prokaryotic homologue of tubulin, plays an essential role in cell division. FtsZ is a potential drug target, as illustrated by the small-molecule cell-cycle inhibitor and antibacterial agent PC190723 that targets FtsZ. We demonstrate that PC190723 negatively modulates *Staphylococcus aureus* FtsZ polymerization cooperativity as reflected in polymerization at lower concentrations without a defined critical concentration. The crystal structure of the *S. aureus* FtsZ-PC190723 complex shows a domain movement that would stabilize the FtsZ protofilament over the monomeric state, with the conformational change mediated from the GTP-binding site to the C-terminal domain via helix 7. Together, the results reveal the molecular mechanism of FtsZ modulation by PC190723 and a conformational switch to the high-affinity state that enables polymer assembly.

Filamenting temperature-sensitive mutant Z (FtsZ) forms filaments that localize to the bacterial cell-division site to form the Z-ring, recruiting other cell-division factors and providing constricting force during cell division.[1] The binding and hydrolysis of nucleotides by FtsZ plays a key role in regulating Z-ring dynamics.[2,3] FtsZ is an attractive drug target for the control of infectious disease given the essential role of FtsZ in the bacterial cell cycle.[4−7] Several small-molecule FtsZ inhibitors have been reported that exhibit antibacterial activity,[2−8] including the small-molecule cell-division inhibitor PC190723 that exhibits antibacterial activity against methicillin- and multidrug-resistant *Staphylococcus aureus* and stabilizes FtsZ filaments.[9,10]

Cooperativity is encountered in numerous contexts in biochemistry. In terms of FtsZ assembly, cooperativity is reflected in assembly occurring with a lag phase followed by a steep transition from monomer to polymer above a characteristic monomer concentration called the critical concentration.[1] FtsZ assembles cooperatively in the presence of GTP (guanosine triphosphate)[11,12] whereas FtsZ does not assemble cooperatively in the presence of GDP (guanosine diphosphate) alone, which induces depolymerization.[11]

The cooperative assembly of multistrand filaments can arise from both longitudinal and lateral subunit contacts, as in the case of tubulin.[13,14] However, the FtsZ protofilament is only one subunit thick, which precludes lateral contacts as a source of assembly cooperativity.[1,12] The cooperative assembly of single-stranded protofilaments has been proposed to arise from either lateral contacts made upon annealing of the ends of a complete single stranded circle[15] or two monomer conformational states with low and high affinities for filament formation.[1,12,16] In the latter model, monomers that adopt a high-affinity conformation are populated at vanishingly small levels until the critical concentration is reached, at which point sufficient nucleation sites exist for elongation to occur. A conformational change to the high-affinity state can explain cooperativity if a binding event at one oligomerization interface is propagated through the monomer to a second oligomerization interface, which is then primed for interaction with an adjacent monomer of the propagating filament. All FtsZ crystal structures to date from several bacteria in the presence of GDP or GTP adopt an essentially identical conformation,[17] presumed to be the low affinity conformation of the allosteric cooperativity model.[18]

GTPase activity provides a surrogate measure of polymerization since the GTPase active site is formed between consecutive monomers upon polymerization.[19,20] Accordingly, the point of maximum GTP-dependent *S. aureus* FtsZ polymerization monitored by light scattering, which reflects filament formation, coincides with the maximum rate of GTPase activity at each FtsZ concentration (Figure 1a). A FtsZ concentration-dependent lag phase, predicted by kinetic models of allosteric cooperativity,[16] is observed prior to the onset of polymerization and GTPase activity (Figure 1a).

GDP induces the depolymerization of FtsZ,[11] and if the depolymerization occurs via stabilization of the low-affinity monomeric state then GDP would be expected to also modulate the cooperativity of GTP-dependent FtsZ assembly. Experimentally, this would be reflected by an increase in both the lag phase and critical concentration.[1,12,16] Indeed, the presence of GDP increases the lag phase of GTP-dependent FtsZ assembly from 5 to 10 min (Figure 1b) and the critical concentration from 4.0 ± 0.1 to 5.2 ± 0.2 μM.[21] (Figure 2a) A classical measure of cooperativity in enzyme kinetics is the Hill slope, with a value of 1 reflective of no cooperativity. The equivalent metric here would be the slope of the transition from monomer to polymer. The transition slope can be monitored by the development of GTPase activity (Figure S1,

Received: April 13, 2012
Published: July 13, 2012

   dx.doi.org/10.1021/ja303564a | J. Am. Chem. Soc. 2012, 134, 12342−12345

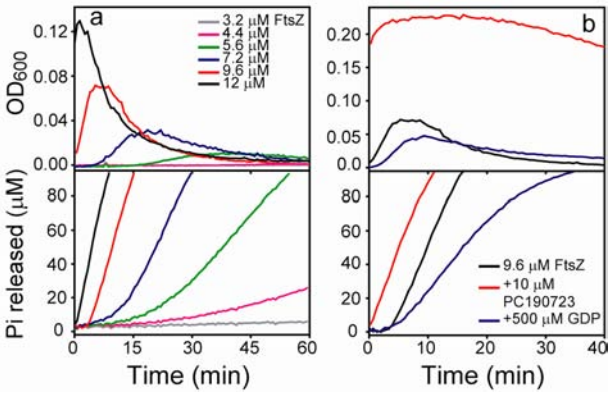

Figure 1. Relationship between GTPase activity and polymerization and the effect of GDP and PC190723 on the lag phase of assembly. (a) GTP-dependent polymerization and GTPase activity display a FtsZ-concentration dependent lag phase. In each assay the maximal rate of GTPase activity in the presence of 500 μM GTP occurs at the peak of polymerization. (b) At 9.6 μM FtsZ, addition of 500 μM GDP decreases the relative polymerization and rate of GTP hydrolysis and increases the lag phase. In contrast, PC190723 abolishes the lag phase, increases the extent of polymerization reflected by light scattering and the rate of GTP hydrolysis. The dramatic increase in light-scattering induced by PC190723 reflects the bundling of FtsZ protofilaments.[10]

Supporting Information), and GDP increases the slope from 4.7 ± 0.3 for FtsZ alone to 8.2 ± 0.7 (Figure 2b). Thus, GDP acts as a positive modulator of FtsZ assembly cooperativity, as reflected in the increased lag time, critical concentration and transition slope.

PC190723 induces opposite effects to GDP on FtsZ polymerization. PC190723 causes a decrease in the concentration-dependent lag phase of polymerization from 5 to <1 min (Figure 1b). In addition, there is no longer a clear critical concentration in the presence of 10 μM PC190723. Instead, GTPase activity is detected at the lowest FtsZ concentration tested (0.4 μM) and increases in an isodesmic fashion (Figure 2a,c). The results are strikingly similar to theoretical plots of cooperativity with the sharpness of the critical concentration for polymerization corresponding to the degree of cooperativity.[12,16] PC190723 causes a concentration-dependent decrease in the transition slope for polymerization (Table S1, Supporting Information, Figure 2c) and as PC190723 approaches saturation the transition slope approaches 1, a value classically considered to be noncooperative (Figure 2b). Thus, PC190723 decreases the cooperativity of GTP-mediated assembly of FtsZ as reflected by a decrease in lag phase, loss of a defined critical concentration, and decrease in transition slope from monomer to polymer.

The estimated intracellular FtsZ concentration is on the order of 10 μM,[23,24] which is comparable to the critical concentration of 4 μM observed here. The decrease in cooperativity caused by PC190723 allows FtsZ to assemble in an isodesmic manner at lower concentrations than required for allosteric assembly. The change in FtsZ assembly mechanism conceivably results in inappropriate FtsZ assembly and disruption of the cell cycle. Indeed, electron microscopy reveals that PC190723 induces FtsZ to form toroids and helical bundles in addition to productive filaments.[10]

Collectively, the biochemical data indicate that PC190723 negatively modulates FtsZ assembly cooperativity. The *S. aureus* FtsZ-PC190723-GDP structure[25] was thus analyzed in the

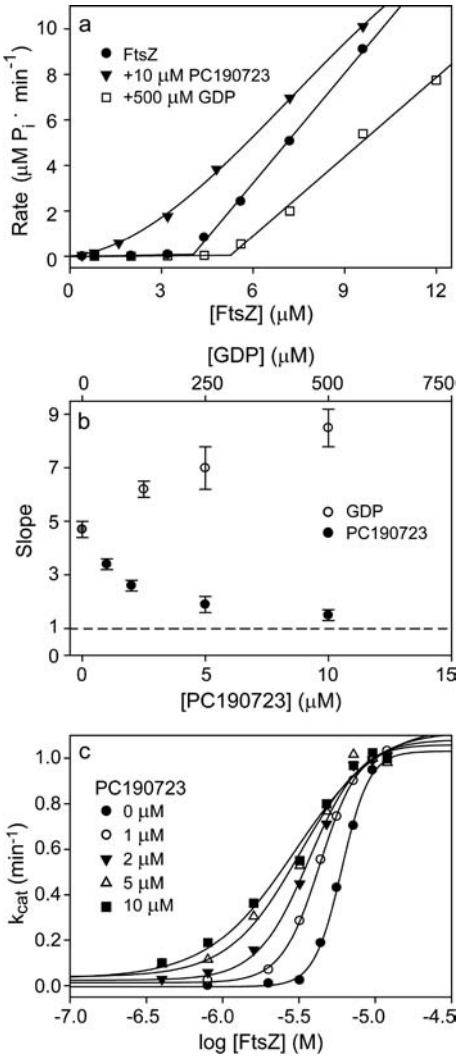

Figure 2. PC190723 decreases GTP-dependent FtsZ polymerization cooperativity in contrast to GDP. For assays with GDP present, the GTP/GDP ratio was held constant at 8:1 to ensure saturating substrate and assembly of FtsZ. All other assays had 500 μM GTP present. (a) GTP-dependent assembly of FtsZ exhibits an unambiguous critical concentration that is increased by GDP. In contrast, PC190723 causes an isodesmic increase in GTPase activity that lacks a well-defined critical concentration in the presence of 500 μM GTP. The line for PC190723 is for illustrative purposes only.[22] (b) Presence of GDP (top axis) increases the transition slope whereas the transition slope approaches 1 as PC190723 (bottom axis) approaches binding saturation. (c) PC190723 decreases the transition slope from monomer to filament in the presence of 500 μM GTP. There exists a mix of cooperative and noncooperative assembly under conditions where FtsZ is only partially bound by PC190723, but in the limit of fully bound FtsZ there will be no cooperativity (reflected by the approach of the transition slope to 1 as the PC190723 concentration increases).

context of protofilament formation. Previously, the structure was described only in terms of the PC190723 binding site and resistance mutations.[25] The structures of FtsZ from five different bacteria in twenty different nucleotide-bound states all adopt essentially the same structure (Figure S2, Supporting Information).[17] In contrast, the FtsZ-PC190723-GDP complex adopts a novel orientation of the N and C-terminal domains that is mediated by helix 7 (Figure 3a). The change in domain orientation results in a change in buried surface area from ~790

dx.doi.org/10.1021/ja303564a | J. Am. Chem. Soc. 2012, 134, 12342−12345

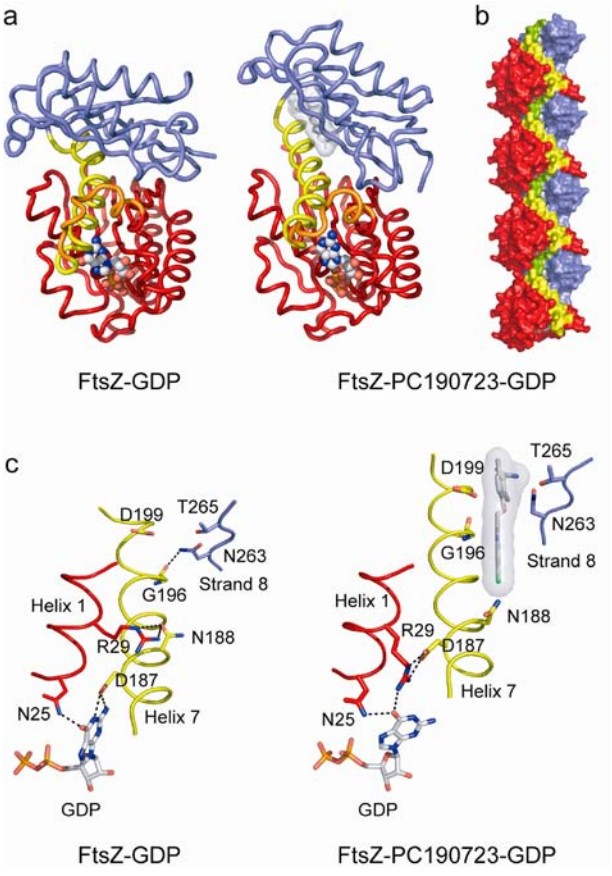

Figure 3. Comparison of the structure of the *S. aureus* FtsZ-PC190723-GDP complex with the structure of the *B. subtilis* FtsZ-GDP complex. (a) Individual N- and C-terminal domains of the *S. aureus* FtsZ-PC190723-GDP structure overlay with *B. subtilis* FtsZ with a C^{α} r.msd (root mean-square deviation) of 0.45 and 0.75 Å respectively but their relative orientation has shifted. The C^{α} r.msd across the entire molecule increases to 1.4 Å. Sequence identity is 80% in the ordered residues of the crystal structure and 100% identity in the nucleotide binding pocket (Figure S3, Supporting Information). (b) FtsZ-PC190723-GDP monomers form an apparent protofilament. (c) Movement of helix 7 provides the conformational trigger from the low to high affinity states.

Å^2 in the FtsZ-GDP structure[26] to ∼1200 Å^2 in the FtsZ-PC190723-GDP complex. This results from previously unobserved interactions between residues on the T7 loop and helix 8 of one subunit with residues in helix 1 of the adjacent subunit. (Figure S3, Supporting Information) The increase in buried surface area would contribute favorably to the stability of the protofilament.

In the crystal lattice, the FtsZ-PC190723-GDP complex adopts a continuous linear head-to-tail arrangement of monomers spaced 43.7 Å apart (Figure 3b), which is consistent with the 40−45 Å subunit spacing of straight protofilaments observed by electron microscopy.[1,10,19] The straight conformation is in marked contrast to the previously observed curved structures of FtsZ.[1,27] The dimer interface completely encloses the bound GDP with the T7 loop blocking access to the binding site and Asp 213 in a position suitable to participate in GTP hydrolysis at a distance of 6.7 Å from the β-phosphate of GDP (Figure S3, Supporting Information).

The trigger for the domain reorientation is provided by helix 7. Helix 7 spans the length of the FtsZ monomer and links the N- and C-terminal domains. In all previous FtsZ structures, helix 7 is anchored to the C-terminal domains by a conserved hydrogen bond between Gly 196 of helix 7 and Asn 263 (or species equivalent) of the C-terminal domain (Figure 3c and Figure S4, Supporting Information). The N-terminal domain is anchored to helix 7 by a conserved hydrogen bond between Asn 188 of helix 7 and Arg 29 of the N-terminal domain, except in *Pseudomonas aeruginosa* FtsZ, in which Arg 29 is replaced with a histidine (Figure S4) and the helix 7 location is maintained by a hydrogen bond involving Asn 32 and Arg 195 instead of Arg 29 and Asn 188.[19]

In the FtsZ-PC190723-GDP structure, the conserved hydrogen bonds involving Arg 29 and Asn 263 are broken as helix 7 moves ∼3.5 Å along the vertical axis away from the nucleotide binding site (Figure 3c). As a result, the entire C-terminal domain is rotated up and away from helix 7 and the N-terminal domain (Figures 3a), creating a groove not present in any previous FtsZ structure, in which PC190723 binds. Thus, PC190723 binds selectively to a novel FtsZ conformation and helix 7 can communicate changes from the nucleotide binding site to the C-terminal domain.

The FtsZ-PC190723-GDP structure reveals a previously unobserved pattern of GDP ligation as a result of the shift in helix 7 and rotation of the C-terminal domain (Figure 3c). Asp 187 on helix 7, previously seen to form a hydrogen bond with the guanine ring of GDP, now forms a salt-bridge with Arg 29. Arg 29, freed of its interaction with Asn 288 due to the helix 7 translocation as mentioned above, moves into the position previously occupied by Asp 187 and forms a hydrogen bond with the C6 carbonyl of GDP. The change in guanine ligation leads to a 30° rotation of the ring relative to the rest of the GDP molecule and may contribute to the communication mediated by helix 7 of the conformational changes at one terminus of a nucleation dimer to the other terminus to form the energy favored state for elongation. The rotation also offers an explanation for the inhibition of FtsZ polymerization observed with C8-substituted GTP analogues.[28] A substituent in the C8 position would sterically clash with the 5′ O of the ribose and preclude the high-affinity FtsZ conformation.

The structural and biochemical data indicate that PC190723 binds only to the high-affinity FtsZ conformation required for elongation. As a result, the free energy of nucleation is lowered by increasing the solution concentration of the high-affinity species, thus decreasing the observed cooperativity manifest in the loss of a defined critical concentration and reduced transition slope for polymerization. The findings substantiate the allosteric cooperativity model of FtsZ polymerization by revealing a second FtsZ conformation in a high-affinity state that allows cooperative protein assembly. Interestingly, PC190723 binds FtsZ between the C-terminal domain and helix 7 in a region analogous to the Taxol binding site of tubulin,[29] with which it appears to share a common mechanism of action by stabilizing the straight conformation and promoting filament assembly.

In conclusion, PC190723 reduces the assembly cooperativity of FtsZ by stabilizing a high-affinity FtsZ conformation that is competent for assembly. Helix 7 communicates the structural change from the nucleotide binding site to the C-terminal domain, thus providing the basis for allosteric assembly. Together, these results reveal a conformational switch that leads to FtsZ polymerization and highlight a novel mechanism of action for the therapeutic modulation of protein activity. The findings also raise the intriguing possibility that designed

dx.doi.org/10.1021/ja303564a | J. Am. Chem. Soc. 2012, 134, 12342−12345

protein molecular machines can be regulated by small molecules.

■ ASSOCIATED CONTENT

Supporting Information

Materials and methods, Table S1 and Figures S1, S2, S3 and S4. This material is available free of charge via the Internet at http://pubs.acs.org.

■ AUTHOR INFORMATION

Corresponding Author

kevin_lumb@merck.com

Notes

The authors declare no competing financial interest.

■ REFERENCES

(1) Erickson, H. P.; Anderson, D. E.; Osawa, M. *Microbiol. Mol. Biol. Rev.* **2010**, *74*, 504−28.

(2) Adams, D. W.; Errington, J. *Nat. Rev. Microbiol.* **2009**, *7*, 642−53.

(3) Romberg, L.; Mitchison, T. J. *Biochemistry* **2004**, *43*, 282−8.

(4) Singh, P.; Panda, D. *Drug News Perspect.* **2010**, *23*, 295−304.

(5) Lock, R. L.; Harry, E. J. *Nat. Rev. Drug Discovery* **2008**, *7*, 324−38.

(6) Awasthi, D.; Kumar, K.; Ojima, I. *Expert Opin. Ther. Pat.* **2011**, *21*, 657−79.

(7) Kapoor, S.; Panda, D. *Expert Opin. Ther. Targets* **2009**, *13*, 1037−51.

(8) Schaffner-Barbero, C.; Martin-Fontecha, M.; Chacon, P.; Andreu, J. M. *ACS Chem. Biol.* **2012**, *7*, 269−77.

(9) Haydon, D. J.; Stokes, N. R.; Ure, R.; Galbraith, G.; Bennett, J. M.; Brown, D. R.; Baker, P. J.; Barynin, V. V.; Rice, D. W.; Sedelnikova, S. E.; Heal, J. R.; Sheridan, J. M.; Aiwale, S. T.; Chauhan, P. K.; Srivastava, A.; Taneja, A.; Collins, I.; Errington, J.; Czaplewski, L. G. *Science* **2008**, *321*, 1673−5.

(10) Andreu, J. M.; Schaffner-Barbero, C.; Huecas, S.; Alonso, D.; Lopez-Rodriguez, M. L.; Ruiz-Avila, L. B.; Nunez-Ramirez, R.; Llorca, O.; Martin-Galiano, A. J. *J. Biol. Chem.* **2010**, *285*, 14239−46.

(11) Caplan, M. R.; Erickson, H. P. *J. Biol. Chem.* **2003**, *278*, 13784−8.

(12) Huecas, S.; Llorca, O.; Boskovic, J.; Martin-Benito, J.; Valpuesta, J. M.; Andreu, J. M. *Biophys. J.* **2008**, *94*, 1796−806.

(13) Rice, L. M.; Montabana, E. A.; Agard, D. A. *Proc. Natl. Acad. Sci. U.S.A.* **2008**, *105*, 5378−83.

(14) Nogales, E.; Wang, H. W. *Curr. Opin. Struct. Biol.* **2006**, *16*, 221−9.

(15) Gonzalez, J. M.; Velez, M.; Jimenez, M.; Alfonso, C.; Schuck, P.; Mingorance, J.; Vicente, M.; Minton, A. P.; Rivas, G. *Proc. Natl. Acad. Sci. U.S.A.* **2005**, *102*, 1895−900.

(16) Miraldi, E. R.; Thomas, P. J.; Romberg, L. *Biophys. J.* **2008**, *95*, 2470−86.

(17) Oliva, M. A.; Trambaiolo, D.; Löwe, J. *J. Mol. Biol.* **2007**, *373*, 1229−42.

(18) Erickson, H. P. *Proc. Natl. Acad. Sci. U.S.A.* **2009**, *106*, 9238−43.

(19) Oliva, M. A.; Cordell, S. C.; Löwe, J. *Nat. Struct. Mol. Biol.* **2004**, *11*, 1243−50.

(20) Löwe, J. *J. Struct. Biol.* **1998**, *124*, 235−43.

(21) Romberg, L.; Simon, M.; Erickson, H. P. *J. Biol. Chem.* **2001**, *276*, 11743−53.

(22) While others have reported an apparent GTPase inhibition by PC190723,[9] the lack of inhibition observed here is consistent with the observation that PC190723 does not interact with the active site in the crystal structure (Figure 3a) and that the active site is correctly formed in the presence of PC190723 (Figure S3, Supporting Information).

(23) Rueda, S.; Vicente, M.; Mingorance, J. *J. Bacteriol.* **2003**, *185*, 3344−51.

(24) Lu, C.; Stricker, J.; Erickson, H. P. *Cell Motil. Cytoskeleton* **1998**, *40*, 71−86.

(25) Tan, C. M.; Therien, A. G.; Lu, J.; Lee, S. H.; Caron, A.; Gill, C. J.; Lebeau-Jacob, C.; Benton-Perdomo, L.; Monteiro, J. M.; Pereira, P. M.; Elsen, N. L.; Wu, J.; Deschamps, K.; Petcu, M.; Wong, S.; Daigneault, E.; Kramer, S.; Liang, L.; Maxwell, E.; Claveau, D.; Vaillancourt, J.; Skorey, K.; Tam, J.; Wang, H.; Meredith, T. C.; Sillaots, S.; Wang-Jarantow, L.; Ramtohul, Y.; Langlois, E.; Landry, F.; Reid, J. C.; Parthasarathy, G.; Sharma, S.; Baryshnikova, A.; Lumb, K. J.; Pinho, M. G.; Soisson, S. M.; Roemer, T. *Sci. Transl. Med.* **2012**, *4*, 126ra35.

(26) Raymond, A.; Lovell, S.; Lorimer, D.; Walchli, J.; Mixon, M.; Wallace, E.; Thompkins, K.; Archer, K.; Burgin, A.; Stewart, L. *BMC Biotechnol.* **2009**, *9*, 37.

(27) The conformation observed for PC190723-GDP-FtsZ bears significant similarity to the subunit orientation of straight tubulin.[29] A detailed analysis will be presented separately.

(28) Lappchen, T.; Pinas, V. A.; Hartog, A. F.; Koomen, G. J.; Schaffner-Barbero, C.; Andreu, J. M.; Trambaiolo, D.; Löwe, J.; Juhem, A.; Popov, A. V.; den Blaauwen, T. *Chem. Biol.* **2008**, *15*, 189−99.

(29) Löwe, J.; Li, H.; Downing, K. H.; Nogales, E. *J. Mol. Biol.* **2001**, *313*, 1045−57.